

# Phase transitions in spin-orbital coupled model for pyroxene titanium oxides

Toshiya HIKIHARA<sup>1\*</sup> and Yukitoshi MOTOME<sup>2</sup>

<sup>1</sup>*Division of Physics, Hokkaido University, Sapporo 060-0810, Japan*

<sup>2</sup>*RIKEN (The Institute of Physical and Chemical Research), Wako, Saitama 351-0198, Japan*

We study the competing phases and the phase transition phenomena in an effective spin-orbital coupled model derived for pyroxene titanium oxides  $ATiSi_2O_6$  ( $A=Na, Li$ ). Using the mean-field-type analysis and the numerical quantum transfer matrix method, we show that the model exhibits two different ordered states, the spin-dimer and orbital-ferro state and the spin-ferro and orbital-antiferro state. The transition between two phases is driven by the relative strength of the Hund's-rule coupling to the onsite Coulomb repulsion and/or by the external magnetic field. The ground-state phase diagram is determined. There is a keen competition between orbital and spin degrees of freedom in the multicritical regime, which causes large fluctuations and significantly affects finite-temperature properties in the paramagnetic phase.

**KEYWORDS:** pyroxene titanium oxides, orbital degree of freedom, Kugel-Khomskii model, spin singlet, dimerization, Hund's-rule coupling, superexchange interaction, field-induced transition, quantum transfer matrix method

## 1. Introduction

It has been recognized that the orbital degree of freedom plays an important role in transition metal compounds.<sup>1-3</sup> The interplay among the orbital, spin, and charge degrees of freedom produces a rich variety of phenomena. In particular, quantum and thermal fluctuations in the competition between the spin and orbital exchange interactions have attracted much interest.

Pyroxene titanium oxides  $ATiSi_2O_6$  ( $A=Na, Li$ ) are typical examples of the systems where the interplay between orbital and spin is expected.<sup>4</sup> In these insulating materials, each magnetic  $Ti^{3+}$  cation has one  $d$  electron in  $t_{2g}$  levels. The lattice structure consists of characteristic one-dimensional (1D) chains of skew edge-sharing  $TiO_6$  octahedra, which are bridged and well separated by  $SiO_4$  tetrahedra. Hence, we can regard the system as a quasi 1D spin-1/2 system.

These pyroxene titanium oxides exhibit a phase transition to the low-temperature phase with a spin gap and a lattice dimerization at  $T \simeq 200K$ ,<sup>4,5</sup> which reminds us of a spin-Peierls transition. However, the magnetic susceptibility shows a peculiar temperature dependence clearly distinct from that of usual spin-Peierls compounds.<sup>4</sup> The magnetoelastic effect is not sufficient to explain the data. Therefore, the other scenario is needed to capture the physics of the transition.

In the previous study, we derived an effective spin-orbital coupled model for the pyroxene compounds in the strong correlation limit of a multiorbital Hubbard model, and investigated it using the numerical method as well as mean-field (MF) analyses.<sup>6</sup> We have shown that the interplay between orbital and spin degrees of freedom plays a decisive role in the spin-singlet formation. In particular, we have found that the system exhibits a nontrivial feedback effect between the orbital and spin correlations: At high temperatures, both correlations are antiferro (AF) type and compete with each other. When

the Hund's-rule coupling is small enough compared to the onsite Coulomb repulsion, the AF spin correlation wins the competition and grows rapidly as temperature decreases. The enhancement of the spin correlation changes the orbital correlation from AF to ferro (F) type, and eventually the F-type orbital correlation causes the spin-singlet formation. The experimental data are explained by the effective model semiquantitatively.

Besides these results, we have also found that there is a chance to realize another type of ordered state in the effective model. Namely, if the Hund's-rule coupling is relatively large, the AF orbital correlation may overcome the AF spin correlation, yielding the spin-F ordered state with AF-type orbital ordering at low temperatures. This result indicates that the model may exhibit a phase transition between the spin-singlet and orbital-F phase and the spin-F and orbital-AF phase by changing the strength of the Hund's-rule coupling.

The aim of this paper is to study the phase transition in the effective spin-orbital model in detail. Using the MF analysis and the numerical quantum transfer matrix (QTM) method, we clarify the nature of the ground-state phase transition and the spin-orbital interplay at finite temperatures in the critical regime. Another purpose of this study is to explore the effect of an external magnetic field on the spin-orbital interplay. We find that the magnetic field also induces the same-type transition.

The paper is organized as follows. In Sec. 2, we introduce the model Hamiltonian. The MF results for the ground state are shown in Sec. 3. There, we also discuss a basic mechanism of the phase transitions. In Sec. 4, we present the numerical results at finite temperatures obtained by the QTM method. Section 5 is devoted to summary and concluding remarks.

## 2. Model Hamiltonian

The microscopic model for the pyroxene compounds has been proposed in Ref. 6. Here, we briefly overview the derivation.

\*E-mail address: hikihara@phys.sci.hokudai.ac.jp

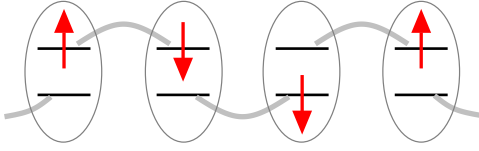


Fig. 1. Schematic picture of the 1D multiorbital Hubbard model for the pyroxene titanium oxides. The ellipses represent Ti sites with doubly-degenerate orbitals, and the gray curves show the  $\sigma$  bonds.

We start from a  $t_{2g}$  multiorbital Hubbard model. In the pyroxene compounds, due to the skew chain structure, the  $\text{TiO}_6$  octahedra are distorted and the threefold  $t_{2g}$  levels are split into a low-lying doublet and a single higher level.<sup>5</sup> It is therefore reasonable to consider the 1D Hubbard model with doubly-degenerate orbitals. For the hopping term, considering the edge-sharing network of  $\text{TiO}_6$  octahedra, we take account of only the  $\sigma$ -bond transfer integrals, i.e., the transfers between the nearest-neighbor (NN) pairs with the same orbitals lying in the same plane, and neglect other small matrix elements. Due to the peculiar zigzag structure of the  $\text{TiO}_6$  chain,<sup>4,6</sup> the NN transfer integrals  $t_{i,i+1}^{\alpha\beta}$ , where  $i$  is site index and  $\alpha, \beta = 1, 2$  are orbital indices, have an alternating form

$$\begin{aligned} t_{i,i+1}^{11} &= t_\sigma \delta_{i,2n+1}, & t_{i,i+1}^{22} &= t_\sigma \delta_{i,2n}, \\ t_{i,i+1}^{12} &= t_{i,i+1}^{21} = 0, \end{aligned} \quad (1)$$

where  $n$  is an integer. The schematic picture of the  $\sigma$  bonds is shown in Fig. 1. As for the onsite interactions, we consider the intra- and inter-orbital Coulomb repulsions  $U$  and  $U'$ , and the Hund's-rule coupling  $J_H$ , which satisfy the relation  $U = U' + 2J_H$ .

From the second order perturbation in the strong-coupling limit  $t_\sigma \ll U, U', J_H$ , the effective spin-orbital Hamiltonian (Kugel-Khomskii type<sup>1</sup>) is obtained as

$$\mathcal{H}_{\text{so}} = -J \sum_i (h_{i,i+1}^{\text{oAF}} + h_{i,i+1}^{\text{F}}) - h \sum_i S_i^z, \quad (2)$$

$$h_{i,i+1}^{\text{oAF}} = (A + B \mathbf{S}_i \cdot \mathbf{S}_{i+1}) \left( \frac{1}{2} - 2T_i T_{i+1} \right), \quad (3)$$

$$\begin{aligned} h_{i,i+1}^{\text{F}} &= C \left( \frac{1}{4} - \mathbf{S}_i \cdot \mathbf{S}_{i+1} \right) \\ &\times \left[ \frac{1}{2} + (-1)^i T_i \right] \left[ \frac{1}{2} + (-1)^i T_{i+1} \right], \end{aligned} \quad (4)$$

where  $\mathbf{S}_i$  is the  $S = 1/2$  spin operator while  $T_i = \pm 1/2$  is the Ising isospin which describes two orbital states at site  $i$ . Note that the orbital isospin interactions are of Ising type because the transfer integrals (1) are orbital diagonal and only one of  $t_{i,i+1}^{11}$  or  $t_{i,i+1}^{22}$  is nonzero on each bond. In Eq. (2), we included the term for the Zeeman coupling with the external magnetic field  $h$  for later use. The coupling constants in Eqs. (2)-(4) are given by parameters in the original multiorbital Hubbard model as  $J = (t_\sigma)^2/U$ ,  $A = 3/4(1 - 3\eta) + 1/4(1 - \eta)$ ,  $B = 1/(1 - 3\eta) - 1/(1 - \eta)$ , and  $C = 4[1/(1 + \eta) + 2/(1 - \eta)]/3$  where  $\eta = J_H/U$ . Hereafter, we set  $J = 1$  as an energy

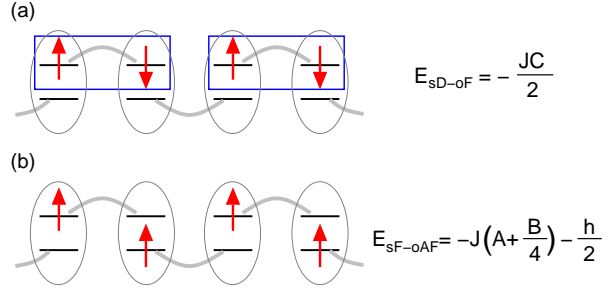


Fig. 2. Schematic picture of (a) the sD-oF state and (b) the sF-oAF state. The rectangles in (a) represent the spin-singlet pairs. The ground-state energies per site are also shown.

unit and use the convention of the Boltzmann constant  $k_B = 1$ .

We note that the JT-type orbital-lattice couplings are also present in real compounds. For the pyroxene compound  $\text{NaTiSi}_2\text{O}_6$ , the JT stabilization energy is estimated to be  $\sim 90\text{K}$ , which is considerably smaller than  $J \sim 200\text{-}300\text{K}$ .<sup>6</sup> In this paper, for simplicity, we consider the 1D spin-orbital Hamiltonian  $\mathcal{H}_{\text{so}}$  only. Indeed, for the realistic value of the JT coupling, the low-temperature properties are dominated by the spin-orbital interplay intrinsic to  $\mathcal{H}_{\text{so}}$ , and the JT coupling just assists to establish the long-range orderings at finite temperatures.<sup>6</sup>

### 3. Mean-field analyses of ground-state phase transitions

#### 3.1 At zero magnetic field

In this section, we consider the ground-state properties of the model (2) at zero magnetic field  $h = 0$  by using a MF-type argument. As discussed in the previous study,<sup>6</sup> we may expect two different types of long-range ordered states in the realistic range of parameters. When the orbital ordering is F-type, *e.g.*,  $\langle T_i \rangle = 1/2$  for all  $i$ , Eqs. (3) and (4) show that the chain is disconnected at every other bonds. The spin-exchange interactions for remaining isolated NN pairs are antiferromagnetic and form the two-site spin-singlet states, resulting in the spin-dimer and orbital-F (sD-oF) ground state [see Fig. 2(a)]. On the other hand, if the orbital ordering is AF type, *e.g.*,  $\langle T_i \rangle = (-1)^i/2$ , the system becomes a uniform ferromagnetic spin chain. Hence, the ground state is the spin-F and orbital-AF (sF-oAF) state [Fig. 2(b)]. Comparing the ground-state energies shown in Fig. 2 at  $h = 0$ , we find that the ground state is sD-oF for  $\eta < \eta_c$  while sF-oAF for  $\eta > \eta_c$ . The critical point is  $\eta_c = (\sqrt{73} - 8)/3 \sim 0.181$ . This transition controlled by  $\eta$  is of first order and accompanied with finite jumps of the spin gap (from  $JC$  to 0) and the magnetization (from 0 to the saturated value  $\pm 1/2$ ).

It should be noticed that the ground-state energies obtained above fully include quantum fluctuations since the orbital interactions are classical Ising type and since the spin ordering is fully polarized F type (no quantum fluctuation) or the two-site singlet state (whose energy is  $-JC$  per singlet pair exactly). In this sense, these results are exact unless an ordering with a period longer than two-site spacing takes place. We will comment on

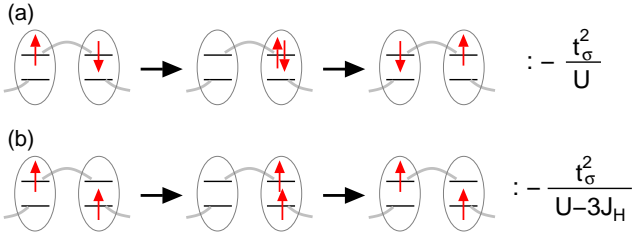


Fig. 3. Schematic picture of typical processes of the virtual hoppings in (a) the sD-oF state and (b) the sF-oAF state. The energy gains for each process are also shown.

the possibility of the ordering of longer period in Sec. 5.

### 3.2 At finite magnetic fields

The transition between the sD-oF and sF-oAF phases is also driven by the external magnetic field  $h$ . The magnetic field suppresses AF spin correlations and favors spin-F state, and hence we may expect a field-induced transition from the sD-oF phase to the sF-oAF phase. Comparing the energies in Fig. 2 including the Zeeman contribution, the critical field  $h_c$  is calculated as

$$h_c = \frac{2(3 - 16\eta - 3\eta^2)}{3(1 - 3\eta)(1 + \eta)(1 - \eta)}. \quad (5)$$

This is also the first-order transition; at the critical point, all the isolated singlet pairs collapse at once, leading to the fully polarized state. We note that the result (5) is also exact in the same sense as that in Sec. 3.1. The phase diagram is shown in Fig. 6 in comparison with numerical results.

### 3.3 Competition between AF superexchange interaction and Hund's-rule coupling

The phase transitions discussed in the preceding sections can be viewed as a result of the competition between the spin-superexchange interaction and the Hund's-rule coupling. The following discussion is sketchy but useful to illustrate the competition. For simplicity, we consider the case without the magnetic field although the discussion is applicable to the case with a finite  $h$ .

Figure 3 shows typical contributions in the perturbation processes to derive the model (2): (a) shows a typical process for the sD-oF configuration, which contributes to the AF spin-superexchange interaction. The energy of the intermediate state is  $U$ . On the other hand, (b) shows a typical process for the sF-oAF configuration, whose intermediate energy is  $U' - J_H = U - 3J_H$ . Hence, the Hund's-rule coupling  $J_H > 0$  tends to enhance the energy gain of the latter process and stabilize the sF-oAF state. We note that the sF-oAF state is indeed favored for any positive Hund's-rule coupling ( $\eta = J_H/U > 0$ ) in the two-orbital model with uniform transfer integrals, i.e.,  $t_{i,i+1}^{11} = t_{i,i+1}^{22} = t_\sigma > 0$  for all NN bonds.<sup>7,8</sup> On the contrary, in the present system, the energy gain by the superexchange process (a) is enhanced in the sD-oF state: Since the alternating transfer integrals (1) break up the system into independent two-site spin-singlet pairs, the ground-state energy for each connected bond is amplified up to  $-JC$ . Moreover, in the AF orbital configurations

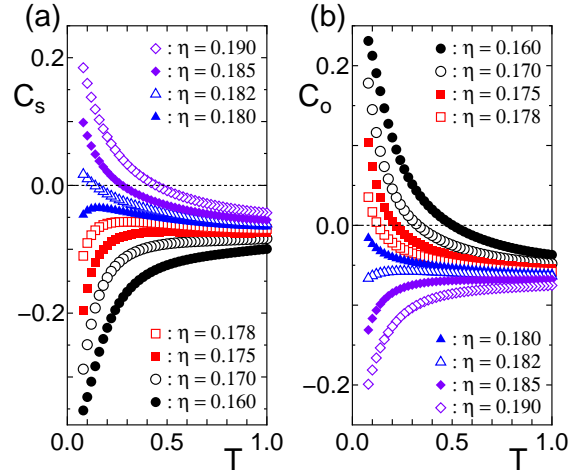


Fig. 4. (a) Nearest-neighbor spin correlation  $C_s$  and (b) the nearest-neighbor orbital correlation  $C_o$  for  $0.160 \leq \eta \leq 0.190$ .

(b), there is no energy gain from the quantum singlet nature because the orbital isospins are of Ising type. These facts give rise to a finite regime of the sD-oF phase for the small values of  $\eta$ .

## 4. Numerical results at finite temperatures

In this section, we present our numerical results for thermodynamic properties of the model (2) obtained by the QTM method.<sup>9,10</sup> Details of the method is described in Ref. 6. In the following, we calculate the NN spin and orbital correlations,  $C_s = \langle \mathbf{S}_i \cdot \mathbf{S}_{i+1} \rangle$  and  $C_o = \langle T_i T_{i+1} \rangle$ , respectively, to clarify the spin-orbital interplay at finite temperatures and the instabilities toward the ground states. The data are for the Trotter number  $M = 4$  and we have checked the  $M$ -convergence of the data.

### 4.1 At zero magnetic field

First, we show the numerical results in the absence of the magnetic field. Figure 4 shows the data of  $C_s$  and  $C_o$  for several values of  $\eta$ . At high temperatures, both spin and orbital correlations are negative, i.e., AF type, and compete with each other. For  $\eta \lesssim 0.180$ , the AF spin correlation wins the competition and yields the sign change of the orbital correlation from AF to F type. After the sign change, both  $C_s$  and  $C_o$  grow cooperatively as temperature decreases, and eventually appear to approach  $C_s = -3/8$  and  $C_o = 1/4$ , the values expected for the sD-oF ground state. On the other hand, for  $\eta \gtrsim 0.182$ , the AF orbital correlation wins the competition and the spin correlation is changed from AF to F type. The correlations appear to converge to  $C_s = 1/4$  and  $C_o = -1/4$  as  $T \rightarrow 0$ , indicating that the system shows the sF-oAF ground state. These results suggest that the ground-state phase transition between the sD-oF and sF-oAF phases occurs at  $\eta = \eta_c \simeq 0.181$ , being consistent with the result of the MF analysis.

It is remarkable that for  $\eta$  close to  $\eta_c$  the competition between the orbital and spin correlations remains serious down to very low temperatures  $T \sim 0.1$ ; both the correlations are gradually *suppressed* as temperature decreases,

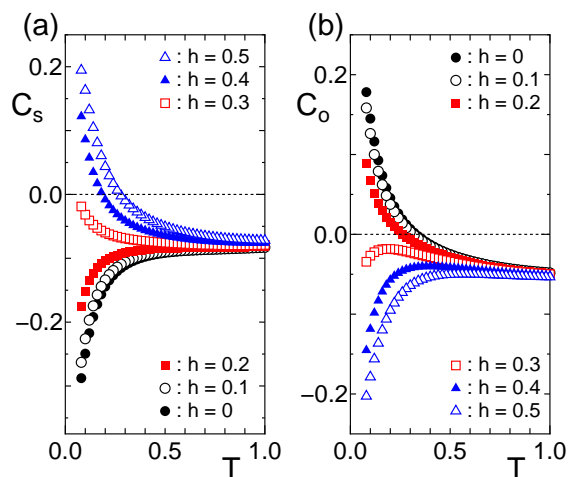


Fig. 5. (a) Nearest-neighbor spin correlation  $C_s$  and (b) the nearest-neighbor orbital correlation  $C_o$  for  $\eta = 0.170$  and several typical values of  $h$ .

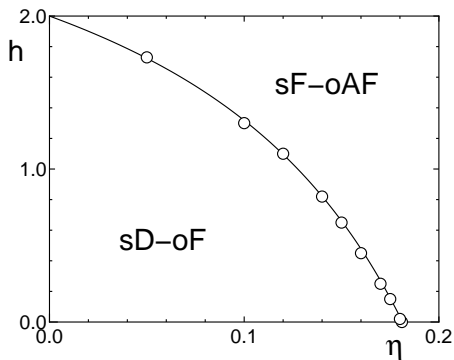


Fig. 6. Ground-state phase diagram in the  $\eta$  versus  $h$  plane. The solid curve represents the mean-field phase boundary [Eq. (5)]. The circles correspond to the transition points estimated by the numerical calculations.

and the convergence to the values expected for the ordered states is not so clear. This peculiar behavior of the correlations indicates that the keen competition between orbital and spin severely affects the finite-temperature properties in the multicritical regime  $\eta \sim \eta_c$ .

#### 4.2 At finite magnetic fields: phase diagram

In Fig. 5, we show the results of  $C_s$  and  $C_o$  for finite magnetic fields at  $\eta = 0.17$ . Similarly to the results in Sec. 4.1, there occurs the transition from the sD-oF phase to the sF-oAF phase by increasing  $h$ , and near the critical field the severe spin-orbital competition survives down to very low temperatures (see the data for  $h = 0.3$ ). We estimate the critical field as  $h_c \sim 0.25$  for  $\eta = 0.17$ , being consistent with the MF result,  $h_c \simeq 0.27$ .

Performing the similar calculations for various values of  $\eta$ , we obtain the ground-state phase diagram in the plane of  $\eta$  versus  $h$  in Fig. 6. The estimates of the critical field by the QTM method agree well with the MF prediction.

## 5. Summary and concluding remarks

We have studied the effective spin-orbital model with alternating couplings [Eq. (2)], which is derived for the pyroxene titanium oxides  $ATiSi_2O_6$  ( $A = Na, Li$ ). Using the MF-type analysis and the numerical QTM method, we have shown that the model exhibits the transition from the spin-dimer and orbital-F phase to the spin-F and orbital-AF phase as the Hund's-rule coupling parameter  $\eta = J_H/U$  increases. The critical value of  $\eta$  is estimated to be  $\eta_c \simeq 0.181$ . Moreover, we have also investigated the effect of the magnetic field  $h$  on the phase transition and determined the phase diagram in the  $\eta$  versus  $h$  plane. The results indicate that the field-induced phase transition occurs in the system with  $\eta < \eta_c$ . We have found a severe competition between orbital and spin degrees of freedom remaining down to very low temperatures near the phase boundary.

As mentioned in Sec. 3, the present MF analysis of the ground state is exact as far as we consider the orderings of two-site period. The QTM results, which can include longer-period orderings, appear to agree well with the MF estimates of the ground-state phase boundary. This agreement suggests that there is no intermediate phase. However, as we noted in Sec. 4, in the critical regime the QTM results are not so conclusive to determine the ground state because of the lack of very low-temperature data; there the QTM method suffers from systematic errors due to the finite Trotter number, and the accuracy is assured for  $T \gtrsim 0.07$  in the present study. Therefore, it is not ruled out to have novel phases in the narrow critical region. This interesting issue is left for future study.

It is a challenging problem to observe the field-induced transition experimentally. The critical field  $h_c$  becomes large as  $\eta$  deviates from  $\eta_c$ ; from the estimate of  $J = 200$ -300K,  $h_c$  reaches 30-50T at  $\eta = 0.175$ . Therefore, to observe the transition in the experimentally accessible range of the magnetic field, it is needed to synthesize a compound with  $\eta$  smaller than but close to  $\eta_c$ . Once an appropriate compound is prepared, one may observe an abrupt change of the magnetization at  $h_c$ , from zero to the saturated value.

## Acknowledgment

We would like to thank M. Isobe and H. Seo for fruitful discussions. This work is supported by NAREGI.

- 1) K. I. Kugel and D. I. Khomskii: Sov. Phys. Usp. **25** (1982) 231.
- 2) Y. Tokura and N. Nagaosa: Science **288** (2000) 462.
- 3) M. Imada, A. Fujimori and Y. Tokura: Rev. Mod. Phys. **70** (1998) 1039.
- 4) M. Isobe, E. Ninomiya, A. Vasil'ev and Y. Ueda: J. Phys. Soc. Jpn. **71** (2002) 1423.
- 5) E. Ninomiya, M. Isobe, Y. Ueda, M. Nishi, K. Ohoyama, H. Sawa and T. Ohama: Physica B **329-333** (2003) 884.
- 6) T. Hikiyara and Y. Motome: to be published in Phys. Rev. B [preprint (cond-mat/0404730)].
- 7) L. M. Roth: Phys. Rev. **149** (1966) 306.
- 8) S. Inagaki and R. Kubo: Int. J. Magnetism **4** (1973) 139.
- 9) H. Betsuyaku: Phys. Rev. Lett. **53** (1984) 629.
- 10) H. Betsuyaku: Prog. Theor. Phys. **73** (1985) 319.